ANL-5893
Metallurgy and Ceramics
(TID-4500, 14th Ed.)
AEC Research and
Development Report

ARGONNE NATIONAL LABORATORY
P. O. Box 299
Lemont, Illinois

NONDESTRUCTIVE TESTING OF EBR-I MARK III FUEL ELEMENTS AND COMPONENTS

by

W. N. Beck, C. J. Renken,
R. G. Myers, and W. J. McGonnagle

Program 7.2.19

May, 1959

Portions of the material in this report have appeared in the following Metallurgy Division Quarterly Reports:

ANL-5709 (18), Oct., Nov., Dec., 1956
ANL-5717 (39), Jan., Feb., Mar., 1957
ANL-5790 (25,26) April, May, June, 1957
ANL-5797 (24-25), July, August, Sept., 1957

Operated by The University of Chicago
under
Contract W-31-109-eng-38

DISCLAIMER

TABLE OF CONTENTS

LIST OF FIGURES

LIST OF FIGURES

NONDESTRUCTIVE TESTING OF EBR-I MARK III FUEL ELEMENTS AND COMPONENTS

W. N. Beck, C. J. Renken,
R. G. Myers, and W. J. McGonnagle

ABSTRACT

Ultrasonic and eddy current methods were used to inspect EBR-I Mark III fuel elements and components. Ultrasonic techniques were used to inspect for: (a) homogeneity of the casting, (b) bonding of the core to the clad on the extruded rod, (c) bonding of the Zircaloy spacer disk to the uranium, and (d) cracks in the Zircaloy rod used for end caps. Eddy current techniques were used to measure the cladding thickness on the extruded rods and to inspect the zirconium wire used for spacers on the completed fuel element.

I. INTRODUCTION

The fuel elements for the EBR-I Mark III core consists of three uranium-2 w/o Zircaloy[1] cylinders, 0.364 inch in diameter, arranged in a line on a common longitudinal center. They were made by the coextrusion process[2] and were clad with a metallurgically bonded Zircaloy-2 cladding, 0.020 inch in thickness. The top and bottom sections, 7.750 and 3.562 inches long, respectively, contain natural uranium only. These act as blanket material above and below the highly enriched uranium fuel section, 8.500 inches long. A 0.010-inch thick Zircaloy spacer at each end of the enriched uranium separates the fuel from the blanket sections. The bottom end of the fuel rod was sealed with a Zircaloy-2 tip having machined triangularly shaped sections which located and oriented the rod when in the reactor. The uranium was sealed at the top end by a short section of zirconium tube which is drilled and taped to receive a stainless steel handle.[4]

The design of the blanket rod uranium section was identical to that of the fuel rods, except that no fuel section is employed. Each rod was made up of one section of Zircaloy-2 clad normal U-2 w/o Zr alloy, 19.852 inches long.

The natural uranium castings for the fuel and blanket elements were made in two diameters: 1.65 inches and 2.5 inches.[3] The smaller diameter castings varied from 9 to 11 inches in length and weighed approximately 5 kg, while the larger castings varied in length from 15 to 18 inches and weighed approximately 8.5 kg.

An ultrasonic transmission technique was used to test the homogeneity of the castings after they had been heat treated and the taper had been removed. Ultrasonic techniques were also used to determine (1) the bonding of the core to the clad on the extruded rod, (2) bonding of the spacer to the uranium, and (3) the detection of cracks in the Zircaloy rod used for the end caps.

Eddy current techniques were used to measure the cladding thickness of the extruded fuel rod. Since measurements required relatively great sensitivity, an instrument which provided a means to compensate for varying probe-to-metal spacing was developed.

The wire spacers on the completed fuel element were welded into place. The welding process required a wire which was uniform and mechanically sound so that a good weld could be produced at each spot and consequently the wires had to be fairly free of cracks and voids. After each wire was welded in place, part of it was removed by a machining process. If cracks existed in the wire the machining process often split it along the crack and damaged the fuel element. An eddy current instrument was developed for determininig the quality of the zirconium wire.

II. ULTRASONIC TESTING

A. Ultrasonic Testing of Uranium Alloy Castings

In order to assure the integrity of the core material of the EBR-I Mark III fuel elements, an ultrasonic test was used to inspect all normal uranium castings for defects in the rough machined condition. A two-crystal transmission technique at an ultrasonic frequency of one megacycle was used. The principle employed in the ultrasonic inspection technique has been described in reference (5).

1. Description of Equipment

The inspection of the castings was performed in a $4\frac{1}{2}$-foot tank scanner. A heavy-duty roller assembly was placed in the tank for supporting and rotating the uranium castings, as shown in Figure 1. The rollers were powered by a "V" belt drive coupled to a motor, the speed of which could be varied. The two inspecting ultrasonic transducers were mounted to a yoke assembly which was attached to the scanner carriage. This carriage provided the translatory motion for the transducers. The transducers were aligned so that the pulsed one-megacycle energy was transmitted through the center of the casting, to insure that the entire cross section of the casting was inspected.

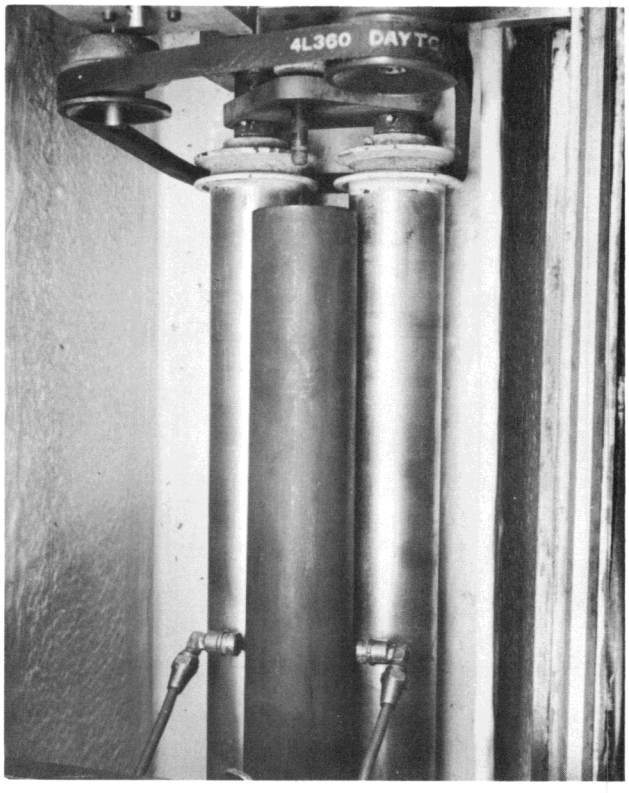

Figure 1
EBR-I Mark III Casting Mounted on Roller Assembly. The two inspecting transducers can be seen in left section of photo.

With the combined rotational motion of the casting and the horizontal travel of the transducers, the composite motion produced a helical scan, the effective pitch of which could be varied. For this test, the rotational speed was preset at one revolution per second. The translational speed of the carriage was adjusted so that, with transducers of 1/4-inch diameter, an overlap of 1/16 inch could be obtained.

The motions of the scanner were synchronized with a helix recorder which transcribed one line on the electrosensitive paper for each rotation of the casting.(5) The paper feed of the recorder was set to displace an equal length of recording paper for the distance traveled by the transducers. The recorded trace was therefore a plane, graphic presentation of the ultrasonic transmission.

The ultrasonic circuitry consisted of a freely running blocking oscillator which pulsed a 1-megacycle barium titanate transducer at approximately 1000 cycles per second.(6) By means of a gate circuit and a current amplifier, the received ultrasonic energy could be amplified, discriminated and recorded on electrosensitive paper.

2. Test Procedure

In order to correlate the recorded information with the defects in the material, a casting was selected at random and several recordings were made at various levels of sensitivity. This casting was then sectioned, polished and inspected. The type of defect which was considered detrimental can be seen in Figure 2. The transverse cut from the top of the castings revealed an area of shrink which extended into the casting for a distance of approximately 1.3 to 2 inches. The gate level of the ultrasonic equipment was then preset so that this defect would be recorded. A photograph of two recorded traces can be seen in Figure 3. The trace on the left indicates by the white spots and lines the presence of shrink areas. The trace on the right shows a casting free from shrink area. From the trace it was also possible to determine the approximate depth of the defect. By virtue of the fact that the inspecting crystals were positioned so that the transmitted ultrasonic energy passed through the middle of the casting, any defect centrally located would attenuate the energy during the complete revolution of the casting. An example of this can be seen as white bands in trace H483-8 of Figure 3. If the flaw was not centrally located, the attenuation would occur only during the time the revolving flaw passed before the inspecting crystals. This image would be repeated on the trace, since the flaw was viewed twice for every revolution of the casting.

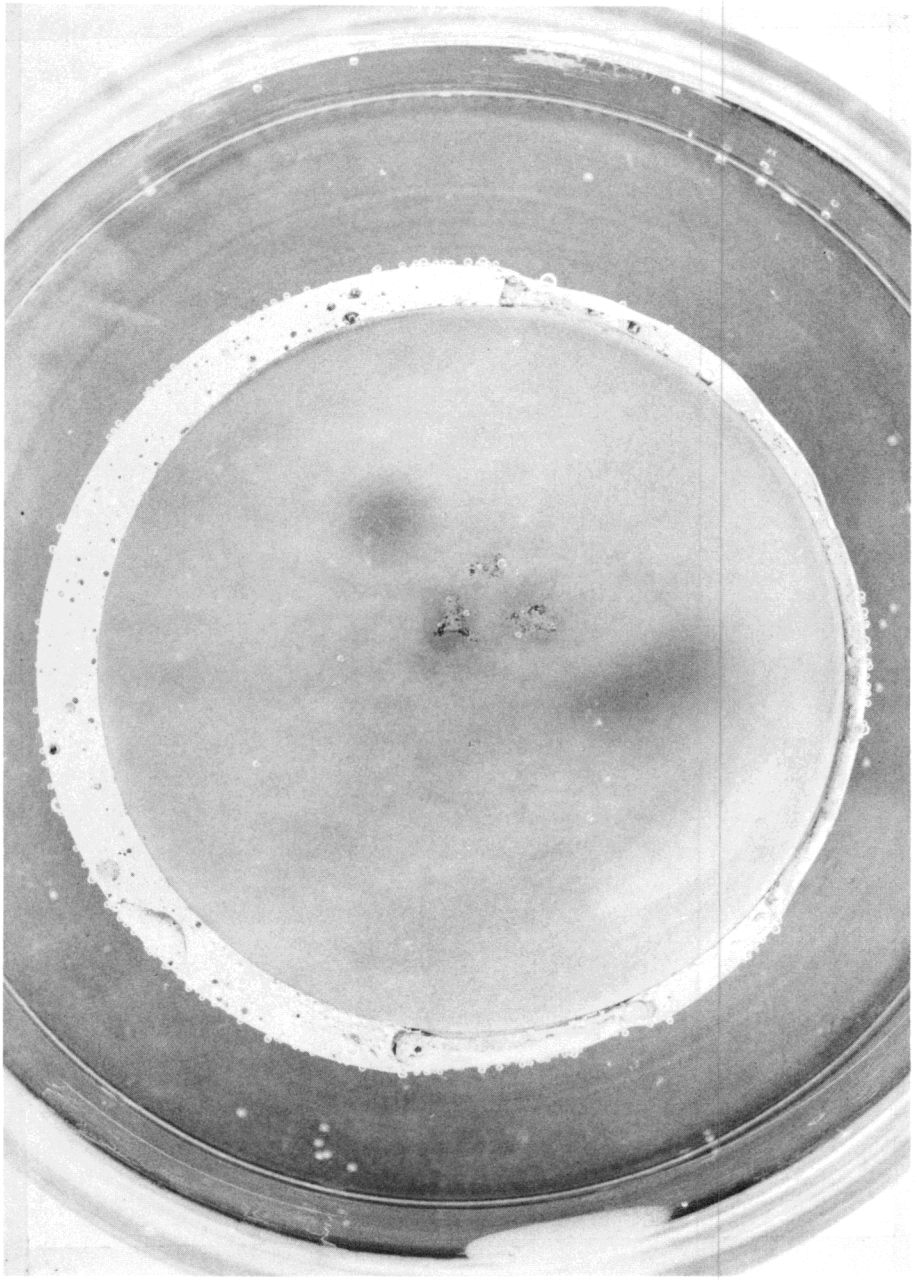

Figure 2

Cut-away Section of Casting Showing
Shrink Area in Center of Casting.

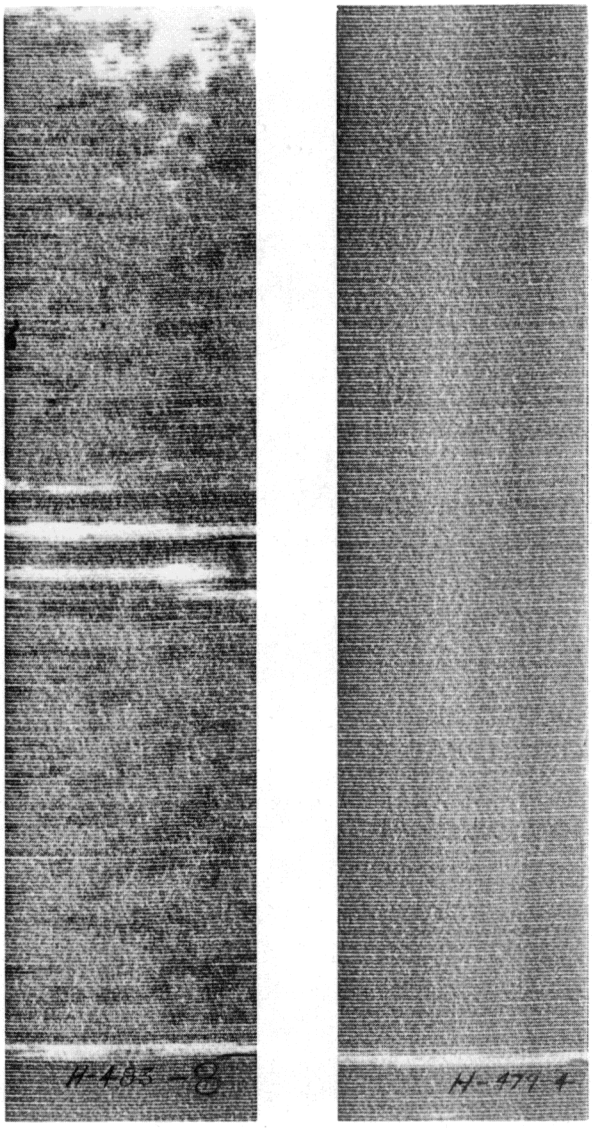

Figure 3

Recorded Traces of Two Castings. Trace at left indicates by white spots and lines the presence of shrink areas. Trace at right indicates sound casting. The white band near the bottom of the trace indicates the end of the billet.

3. Test Results

In the development and quality control program, a total of 109 castings were tested. The ultrasonic technique as applied in this test provided an accurate and rapid means of locating shrink and porosity in the castings. The selected scanning speed was not representative of the maximum rate of processing, for the equipment was successfully operated with the casting rotating at 4 revolutions per second.

B. Ultrasonic Tests of Fuel Elements

In order to determine that the Zircaloy clad had firmly adhered to the core, the extruded fuel and blanket rods were inspected using ultrasonics. The technique applied was an immersed transmission technique at a frequency of 5 megacycles.

1. Description of Test Equipment

To test the fuel and blanket rods a double roller feed assembly was designed and fabricated as shown in Figure 4. The roller assembly measured 3 feet in length, 8 inches in width and 6 inches in height. The rollers were 3-inch, rubber-tired aluminum wheels, arranged in two rows. Each pair of diametrically opposed rollers were mounted on one common swivel bracket. All the brackets were ganged to one longitudinal shaft so that the relative angle of the rollers with respect to the center line of the assembly could be changed, thus providing a means whereby the effective translational pitch of a specimen mounted on the rollers could be varied. One row of rollers was powered by a common torsion shaft. The other row acted as idlers. Each roller could be independently adjusted to compensate for misalignment. This adjustment feature also made it possible to vary the overall spacing of the rollers so that cylindrical specimens of various diameters could be tested. In operation, the roller assembly was positioned in the tank of the $10\frac{1}{2}$-foot ultrasonic scanner.(5) A belt joined the pulley on the roller assembly to the variable speed output shaft on the scanner. By varying the angle of the rollers and speed of the drive shaft, the translational speed and pitch of the fuel and blanket rod could be preset.

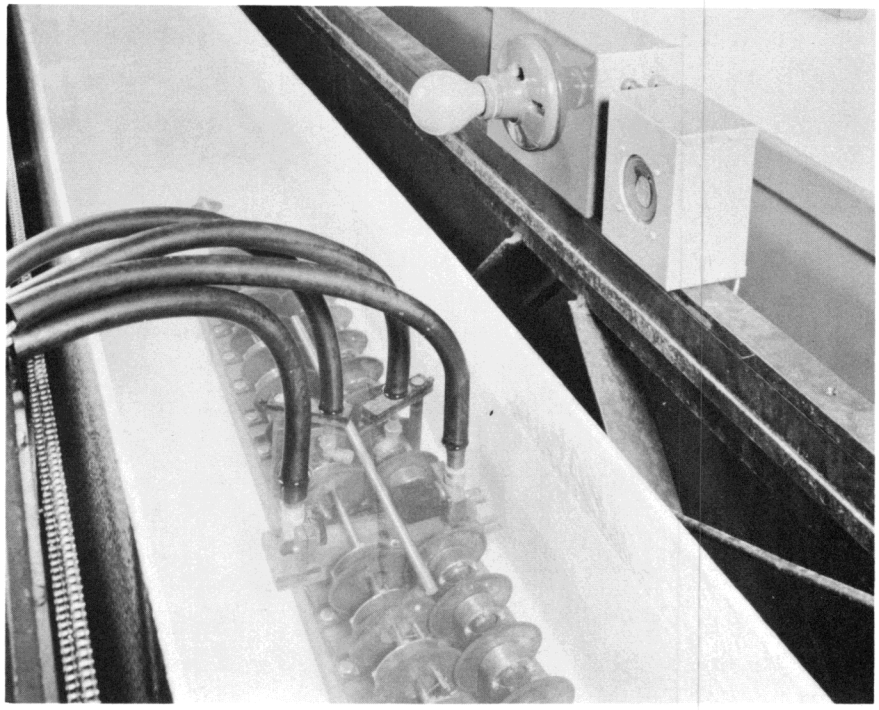

Figure 4

Test Apparatus Showing Roller Assembly Inspecting Transducers and Alarm Systems

2. Core-to-Clad Bond

The ultrasonic transducers were mounted on adjustable pedestals which were affixed directly to the roller assembly platform. Two separate transducers were used, one of which served as a transmitter and the other as a receiver. The transmitting transducer was masked so that the beam aperture measured 5/64 inch in diameter. The ultrasonic circuitry constituted essentially the system described in reference (5). A permanent recording was not made of these fuel elements; instead, an alarm circuit, which provided a 360-cycle audio signal whenever a nonbond area was detected, was devised.

As a means of establishing the resolution for the test, a fuel element with known sizes of defects was made. This was done by drilling the cladding and filling the areas with an absorbent acoustic material. In addition, small random slots were cut into the cladding so as to simulate cracks or breaks.

Using this technique a nonbond area of 1/32 inch could be detected. Repeated scanning tests were made at various rotational, as well as translational, speeds in order to establish the maximum rate of processing. It was determined that the element could be satisfactorily tested if rotated at 188 rpm, with an effective pitch of 0.13 inch, giving a translation rate of approximately 2 feet per minute.

A total of 832 fuel elements were tested for nonbonding. Of this number, three indicated discontinuities in the core-to-clad bond. Since the test was a transmission technique, it was possible to evaluate simultaneously the presence of core cracks or separations in the uranium core. There was no evidence to indicate the presence of such flaws. Inclusions and variations in grain structure were detected in certain elements. These particular defects could be correlated with the casting from which the fuel rod had been made. They were not considered of a nature or magnitude which would adversely affect the integrity of the element and were consequently disregarded.

3. Section Bonding Test

The junctions of individual fuel rod sections were made by a process of heli-arc welding the cladding. A subsequent induction melting of the uranium at the juncture fused the core material to the 0.010-inch Zircaloy spacer. Information regarding the total area which had fused during the induction melting was considered essential. In order to inspect for this, a test, which involved an ultrasonic immersion, two-crystal reflection transmission technique, was devised. The principle of the technique was to impinge an ultrasonic beam at an angle on the section bond. A second transducer was positioned on the opposite side of the specimen so that the

reflected energy at the incident angle from the section bond could be detected. Only the junction which was not bonded presented and reflected the ultrasonic energy at the incident angle. The amount of energy reflected was directly related to the area of the nonbond.

The transducers were pedestal mounted on the roller assembly. The individual holders were made such that each crystal could be adjusted for elevation and angularity. The ultrasonic equipment selected for the test was a 1-megacycle pulsed oscillator.(6) The alarm circuit constituted a relay and light system which provided a visual signal whenever the amplitude of the received impulse exceeded the threshold of a preselected gage.

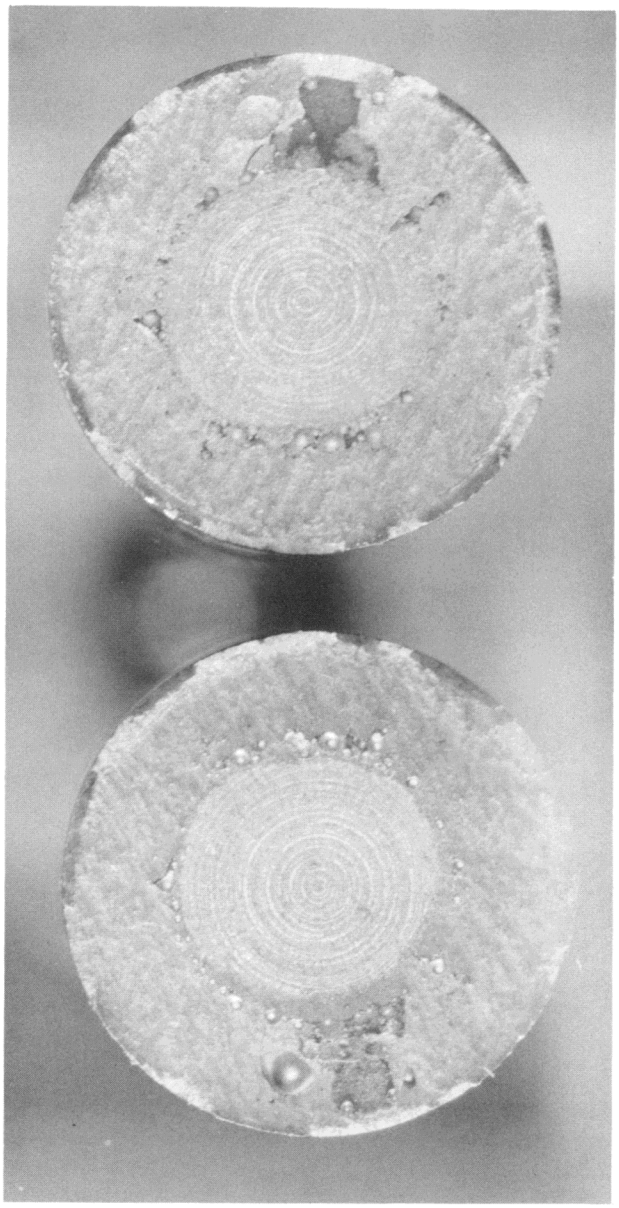

Macro 22166

Figure 5

Section Bond Fracture Revealing a Bonded Interface of Less than 60% Total Area.

As a means of establishing a correlation between the nonbond area and the received ultrasonic energy, several samples of fuel elements, which had purposely been subjected to various melting temperatures by induction heating, were prepared. After the section bonding had been tested and recorded, the junction was fractured and the nonbond area was measured. Figure 5 is a photograph of a section bond interface where less than 60% of the area had fused. The ring effect visible in the middle of the rod is due to a machining operation prior to assembly and welding. In Figure 6 the fused area was greater than 70% and in Figure 7 the area is estimated greater than 80%.

A series of fuel rods was then made, tested and fractured in a tensile testing machine to determine the validity of the test. On the basis of these tensile tests, the optimum minimum bond area was established at 70%,

Macro 22168 4X

Figure 6

Section Bond Fracture Revealing Approximately 70% of Area Bonded.

Macro 22198 6X

Figure 7

Section Bond Fracture Showing Interface Bonding in Excess of 80% Total Area.

which insured a tensile strength of approximately 10,000 psi. With this established minimum, the gate circuit of the ultrasonic equipment was preset so that the visual alarm would be actuated whenever a juncture with less than 70% bond area was presented to the inspecting crystals. A special rod with known nonbond area was retained so that a periodic check on the sensitivity of the equipment could be made.

A total of 2148 section bonds was tested in 837 separate fuel elements. Eighty-three junctures indicated a nonbond area in excess of the prescribed minimum. These particular fuel elements were reprocessed and reinspected. Of these only two failed to meet the specified minimum bonding.

C. Ultrasonic Tests of Zircaloy Rods

The 1½-inch end caps which were welded to fuel-bearing rods were fabricated from extruded Zircaloy rods, 0.403 inch in diameter. In the process of induction welding the caps to the fuel assembly, it was noted that certain caps showed the presence of the star cracks. As a means of detecting this type of defect, the Zircaloy rod was subjected to an ultrasonic inspection. The existing scanning equipment was adapted to the test. The core-to-clad nonbond test crystals were used to detect longitudinal cracks. The section bond test crystals served to detect peripheral cracks. The alarm systems of the two ultrasonic detection units were preset to trip on a sub-surface crack 10 mils in depth. Approximately 100 feet of Zircaloy rod were inspected in this manner. In this test, the roller conveyor was manually operated so as to permit the operator to mark the areas indicating the presence of cracks. Defective areas were cut out of the rods and the remainder used in the manufacture of the fuel elements. Figure 8 shows an enlarged view of cracks in the Zircaloy rod which were detected by this test technique.

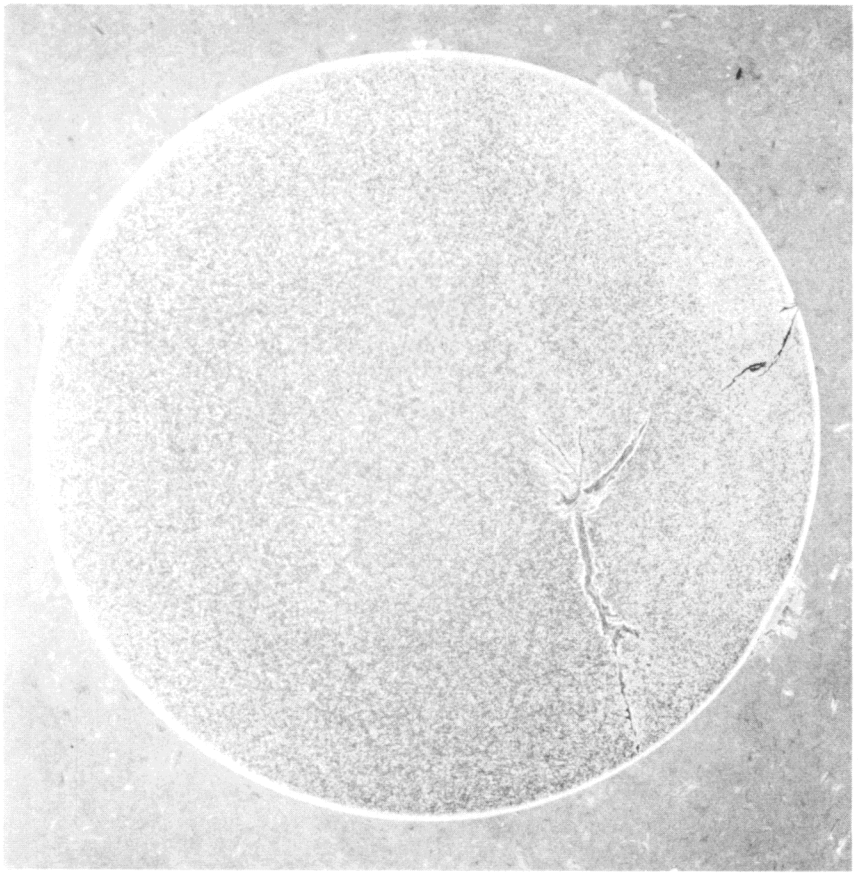

Macro 22469 10X

Figure 8

Cut-away Section of Zircaloy Rod Showing Cracks and Breaks

III. EDDY CURRENT TESTING

A. A Multifrequency Eddy Current Testing System for Measurement of Cladding Thickness

1. Introduction

An eddy current system was developed for the measurement of the thickness of the cladding on the EBR-I Mark III fuel and blanket rods. However, this system has many other applications, such as the measurement of wall thickness of metal tubing with extreme accuracy, and the detection of subsurface cracks and voids in metals.(7) This system has a much greater sensitivity than the system described in Chapter III of ANL-5861.

Eddy currents of two or more separate frequencies are induced to flow in the specimen to be tested. One frequency is used to obtain the information required; the other frequency is used to compensate for the effect of variations in test coil-to-metal spacing and other undesirable effects.

2. An Application of the Dual Frequency System

This test problem required an accurate measurement of the thickness of the Zircaloy-2 clad on EBR-I Mark III fuel elements (0.404 inch in diameter, clad with a nominal 20 mils of Zircaloy-2 on a U-2 w/o Zr core). The resistivity of the core was approximately 72 microhm-cm, while that of the cladding material was in the neighborhood of 52 microhm-cm. Since measurements of this type require relatively great sensitivity, an instrument which does not provide some method of compensation for varying probe-to-metal spacing cannot be used in a production application. It was expected that the cladding thickness would always range between 15 and 25 mils. Experiments showed that frequencies between 25 and 50 kc were suitable for the measurements. It was also determined that eddy currents of a frequency of 260 kc were relatively ineffective for the measurement of clads thicker than 15 mils.

3. Basic Features of the System

It is simpler to consider each channel of the system separately. In the block diagram Figure 9, the elements of each channel are shown according to their function and not necessarily according to position in the circuit diagram. In the high-frequency channel, a sinusoidal voltage of 262 kc is generated and applied across the probe winding. The probe forms part of a bridge circuit which is balanced when the probe is far away from any metal. Any change in the field about the probe causes an

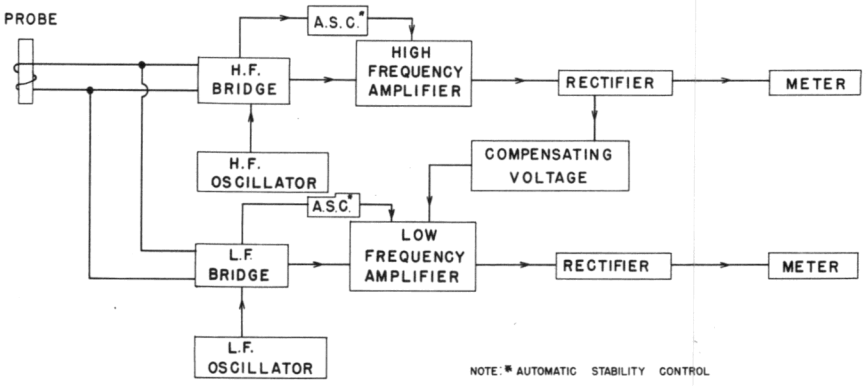

Figure 9

Block Diagram of System

apparent change of the impedance as seen looking into the terminals of the probe. This unbalances the bridge and causes a voltage to appear at its output terminals. Changing the distance from the probe to the metal produces a voltage which is amplified and rectified. Figure 10 shows how this voltage may vary with the spacing from the probe to fuel element.

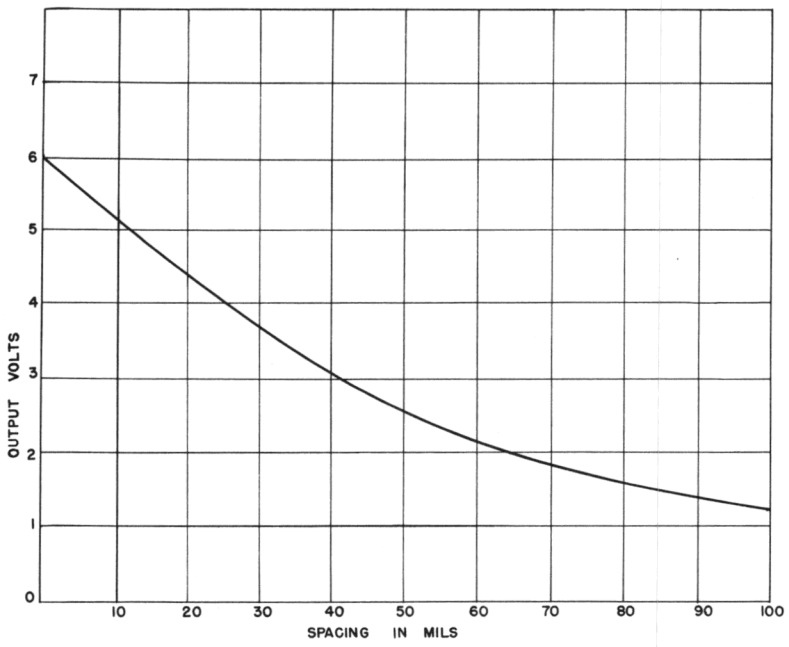

Figure 10

The High-Frequency Channel Output Voltage Plotted as a Function of Probe-to-Metal Spacing

The high-frequency channel output is practically independent of the cladding thickness, since a frequency of 262 kc is too high to be effective for the measurement of the cladding thickness.

All that has been said concerning the high-frequency channel can be said for the low-frequency channel except that it produces a voltage which is a function of the same variables as the high-frequency channel plus an additional variable, the cladding thickness. In addition, the low-frequency channel amplifier is designed so that its gain may be varied by means of a DC voltage which is normally supplied from the high-frequency channel output. The high-frequency channel output voltage varies with probe-to-metal spacing and changes the gain of the low-frequency channel just enough to compensate for the effect of varying probe-to-metal spacing on the low-frequency channel output. Figure 11 shows a typical curve of low-frequency channel output plotted versus distance from a fuel element. The change in low-frequency channel sensitivity produced by a change in cladding thickness from 21 mils to 18 mils is plotted in Figure 12 as a function of probe-to-metal spacing. From Figures 11 and 12 it can be deduced that the voltage produced by the high-frequency channel must compensate for at least two separate effects which could cause an error in the measurement of the cladding thickness. One is the actual change in the magnitude of the low-frequency channel output caused by varying spacing.

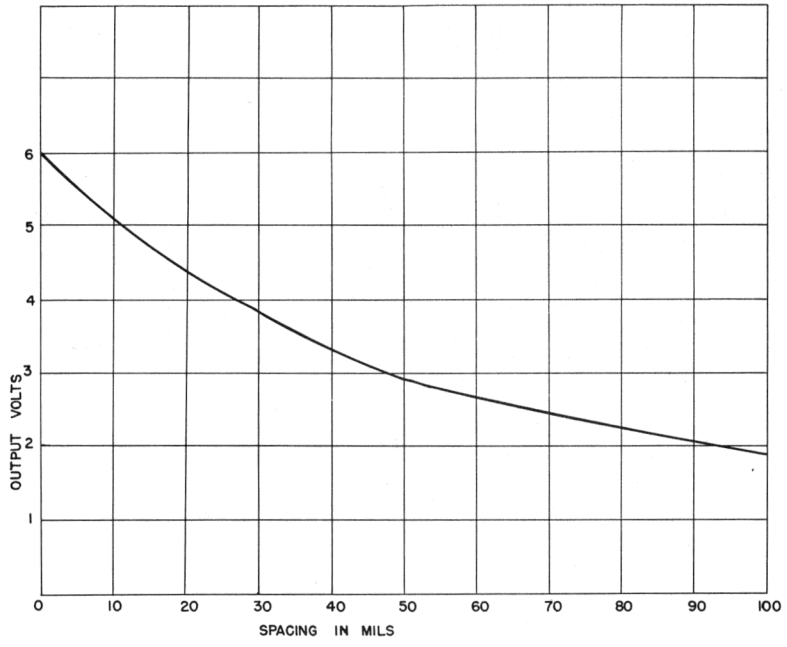

Figure 11

Amplified Low-Frequency Bridge Output Voltage Plotted as a Function of Probe-to-Metal Spacing

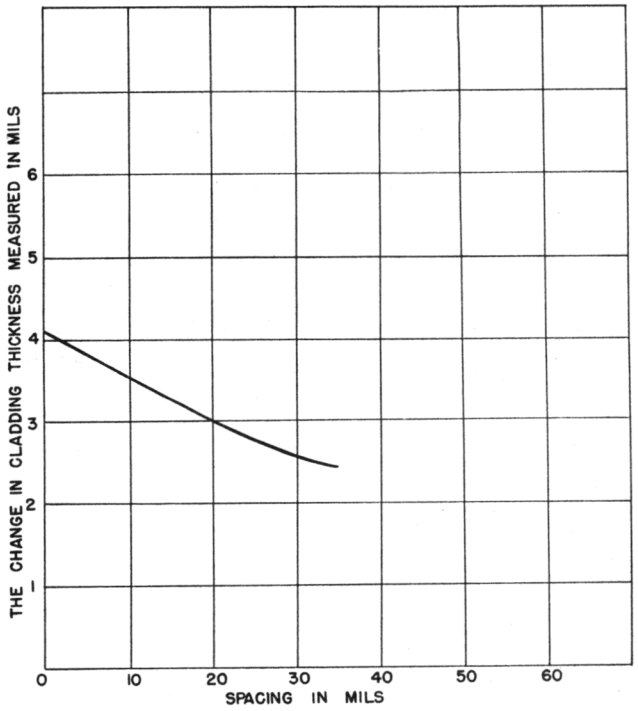

Figure 12

Low-Frequency Channel Sensitivity Plotted as a Function of the Probe-to-Metal Spacing

The other is the dependence upon probe-to-metal spacing of the low-frequency channel sensitivity to a given change in cladding. Figures 13 and 14 show how Figures 11 and 12 look after probe-to-metal compensation has been added. Details of the compensation process are given in Appendix IV of ANL-5861.

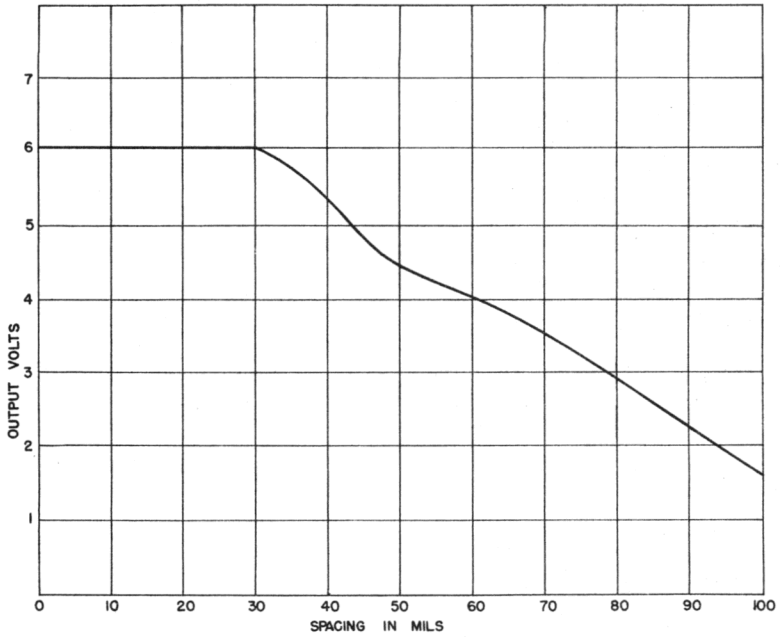

Figure 13

Low-Frequency Channel Output Voltage Plotted as a Function of the Probe-to-Metal Spacing. Compensation Used.

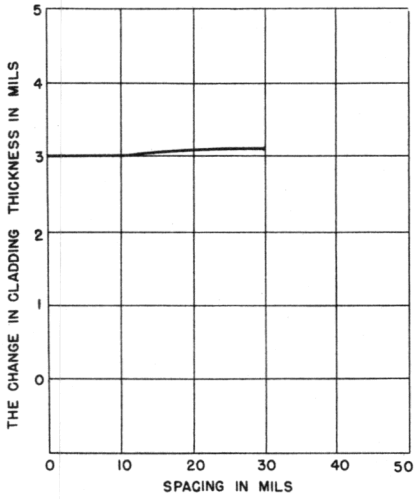

Figure 14

Low-Frequency Channel Sensitivity Plotted as a Function of the Probe-to-Metal Spacing. Compensation Used.

4. Probes

The probes used in this application were wound on 1/4-inch or 3/16-inch cylindrical ferrite forms. The winding consisted of a single layer of #40 enameled wire. Single-layer windings usually possess smaller temperature coefficients of inductance than do multilayer windings. A typical probe is shown in Figure 15 in position over a segment of fuel rod. Probe inductance is not critical; a number of probes of widely different inductances have been used in this particular test problem with no important adjustments necessary, except balance of the bridges and the readjustment of the high and low-frequency channel gains.

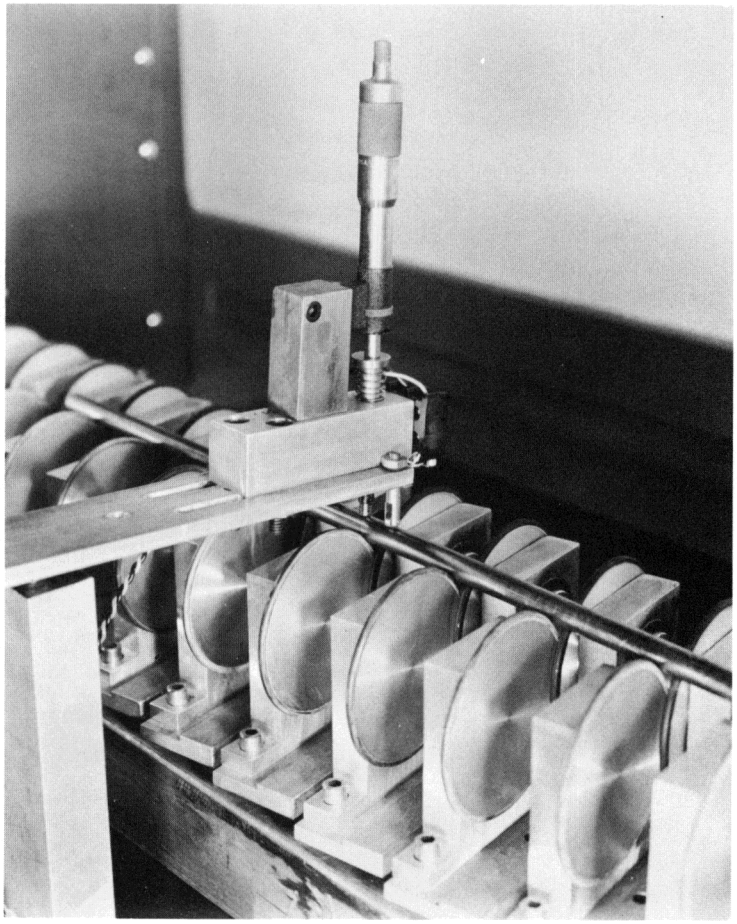

Figure 15

A Typical Probe Shown in Position over a Fuel Rod

5. Circuitry

The circuit diagram of the low-frequency channel is shown in Figure 16, and that of the high-frequency channel in Figure 17. Since the probe is a common element of each bridge, low-frequency voltage is present

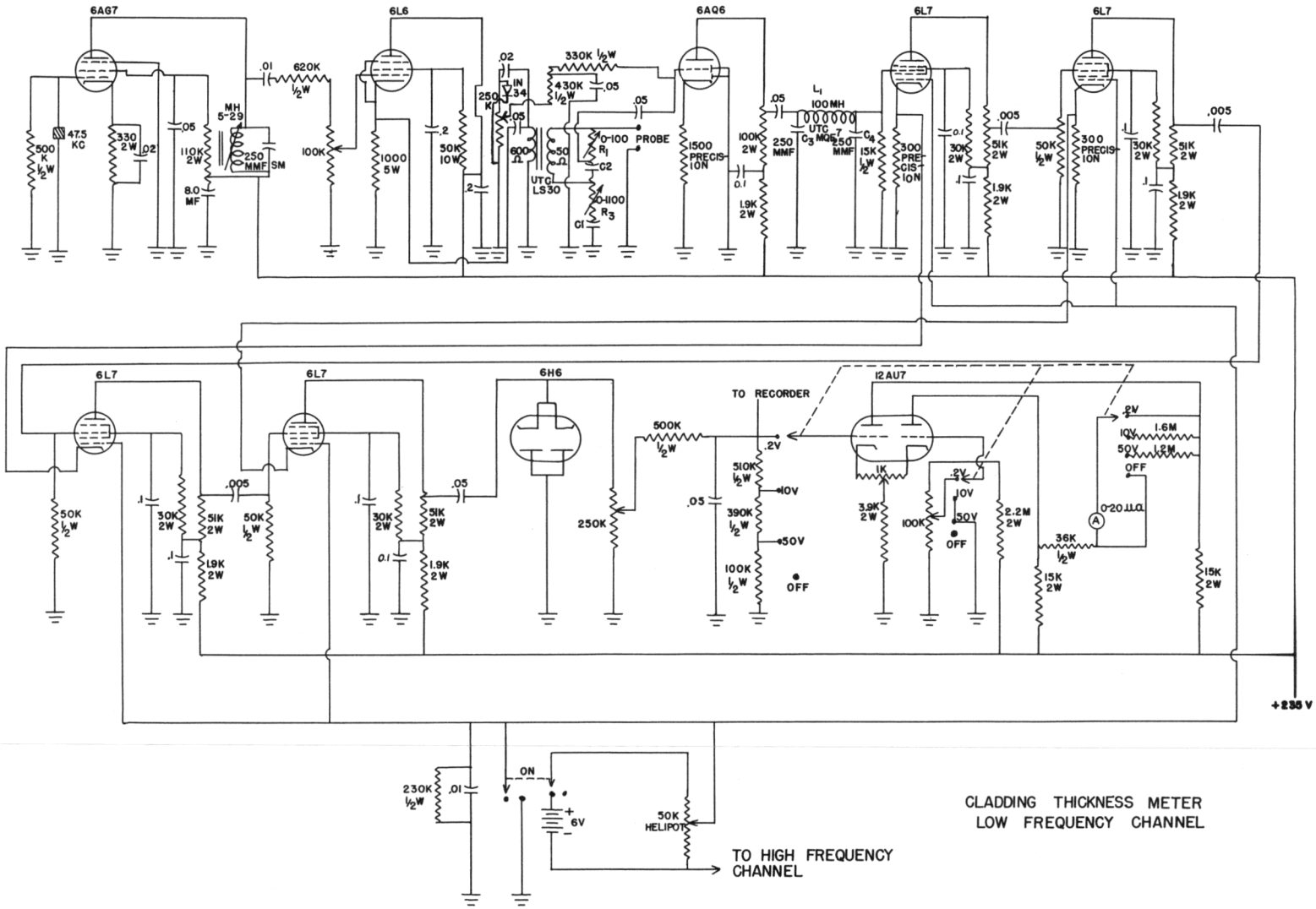

Figure 16

Circuit Diagram of the Low-Frequency Channel

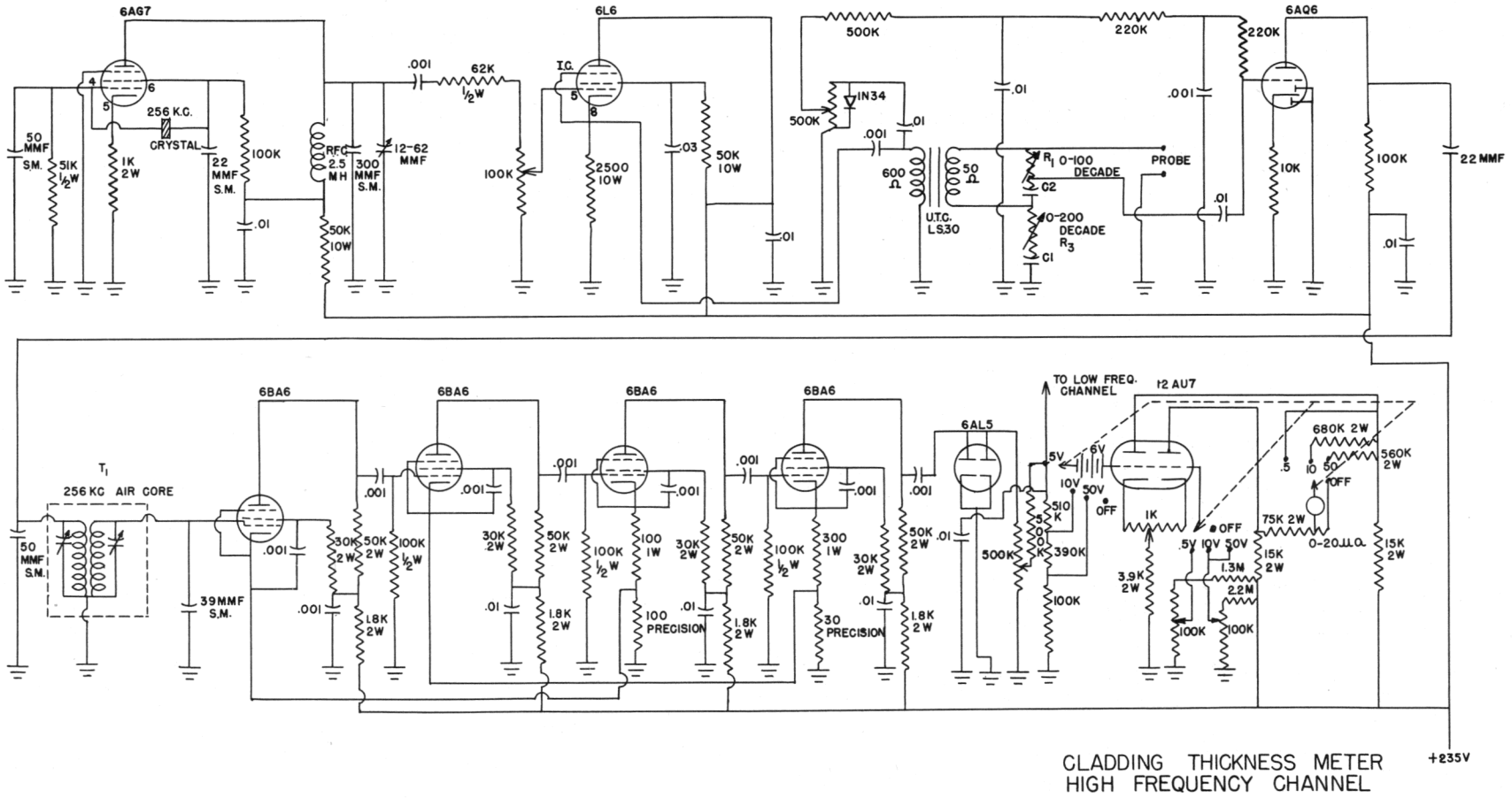

Figure 17

Circuit Diagram of the High-Frequency Channel

in the output of the high-frequency bridge and vice versa. These undesired frequencies must be filtered out. This is done early in the amplifiers since the bridges are not balanced with respect to these frequencies and their relatively high amplitude would overload later stages of the amplifiers. The low-frequency bridge is always balanced first, since it affects the balance of the high-frequency bridge to a large degree, while the reverse effect is only slight. The bridges are balanced by means of the variable resistors R_1 and R_3 in each bridge. The crystal oscillators furnish the sine wave voltages needed to drive the probe. No particular frequency stability is needed; crystals are used in this instrument because the amplifiers in earlier models were sharply tuned. The crystal oscillators have been carried over from the earlier models. RC oscillators have been used successfully. The oscillators should provide voltage of less than 5% distortion. Changes in oscillator output amplitude are compensated by the IN34 diodes in each channel and their associated circuitry. Part of the oscillator output is rectified and fed to the 6AQ6 stage in each channel. Any change in oscillator output changes the gain of this stage so as to maintain the output of the 6AQ6 stage independent of routine variations in oscillator output. The 262-kc voltage is filtered out of the low-frequency channel amplifier by the low pass filter $L_1C_3C_4$. The doubly tuned transformer T_1 performs an analogous function for the high-frequency channel. The output of each channel is fed to separate difference voltmeters with several ranges. Two of the ranges on each voltmeter are useful when balancing the bridges. The most sensitive scale on the low-frequency channel difference voltmeter is calibrated directly in mils of cladding, while the most sensitive scale of the high-frequency channel difference voltmeter is used to keep check on the probe-to-metal spacing. An output from the low-frequency channel can be connected to a recording voltmeter.

6. Mechanical Conveyor

The instrument and conveyor to move the fuel elements past the probe are shown in Figure 18. Skewed wheels, equipped with ribber tires, rotate the rod and at the same time provide it with motion along its longitudinal axis. The pitch of the wheels is set so that every portion of the rod is inspected with some overlap included. No trouble was experienced in maintaining the fuel elements in the proper position for testing as they passed under the probe. Probe-to-metal spacing was easily held within the range over which nearly perfect compensation could be achieved. The probe inspected an area roughly equal to its cross-sectional area, since changes of cladding thickness which lie beyond the projection of the probe on the fuel rod influenced the measurements, while the probe was relatively insensitive to the thickness of the clad which lay immediately beneath its center. Inspection of a fuel element 19.8 inches long required about 30 seconds.

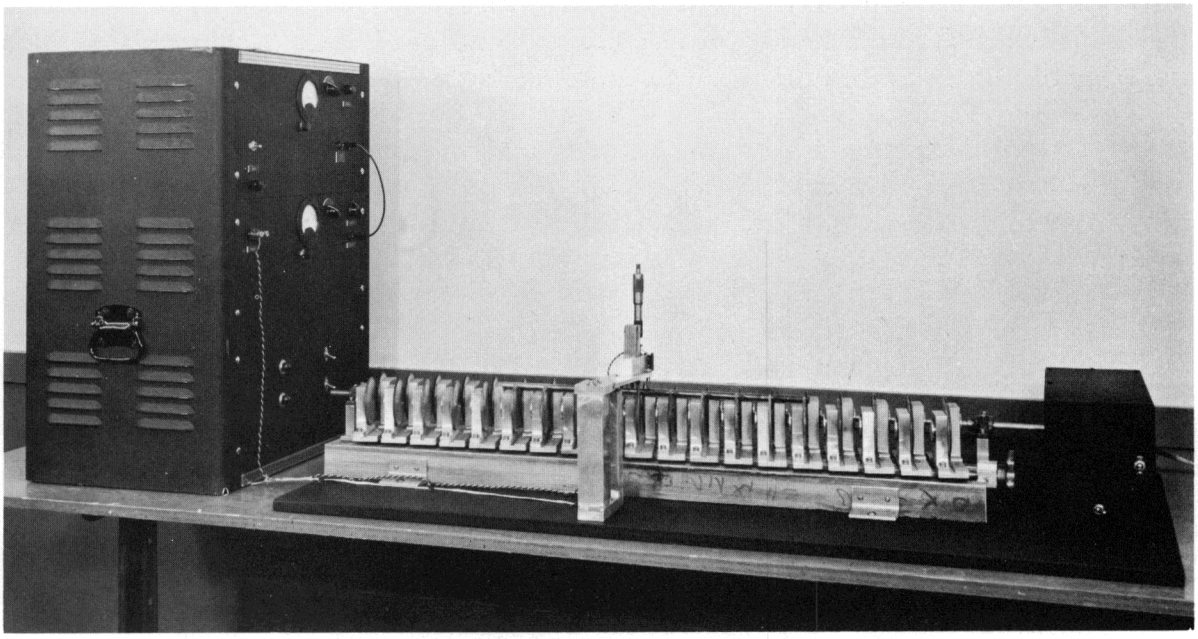

Figure 18

The Complete System

7. Calibration

The calibration of an instrument for nondestructive testing is always one of the most difficult phases of its development. Calibration of this instrument involved the following steps. (1) A certain amount of the cladding was machined from a fuel element; the amount machined off was determined by a measurement of the cladding thickness with a measuring microscope before and after machining. (2) The sensitivity of the instrument was adjusted so that it measured the incremental change correctly, going from the machined part of the fuel element to the unmachined part. Two sources of possible uncertainty arise at this point. The machining creates a standard of a slightly different diameter than the actual rod. However, this amounts to only about 0.8% change in diameter, much too small to cause any significant error, since the instrument compensates for small changes in diameter. The other source of uncertainty arises from the fact that the eddy current measurements cannot be made at the end of the rod because of end effects, while the optical measurements can be made only at the end. So it is necessary to assume that the cladding thickness at a small distance from the end is practically the same as it is at the end. (3) Once the sensitivity of the instrument was adjusted to the proper value, the instrument was used to find a fuel element which possessed very uniform cladding. The cladding on the rod selected varied less than 0.5 mil over the entire length. This rod was sectioned and found to have cladding 21 mils thick. It was used as the standard for all subsequent measurements. It was necessary to apply a 1-mil correction to the

measurements made on rods tested after heat treatment since the heat treatment caused changes to take place in the core material and bond layer which did not exist in the "as-extruded" standard.

Figure 19 shows an actual recording of the cladding thickness of a fuel element near the end of the extrusion. The heavy taper of the cladding made this region particularly suitable for sectioning. Exact comparison between nondestructive measurements and destructive measurements is impossible since the probe measures the average cladding thickness over a certain area while measurements made by the measuring microscope are obtained point-by-point. The oscillations of the trace in Figure 19 were caused by a slight eccentricity of the cladding. The dots shown in the trace indicate the average cladding thickness obtained when measurements were made on the cross section of the rod which lay immediately underneath the centerline of the probe at that time. The average cladding thickness was based on four measurements around the circumference. The probable difference between nondestructive and destructive measurements based on this tape is 0.25 mil.

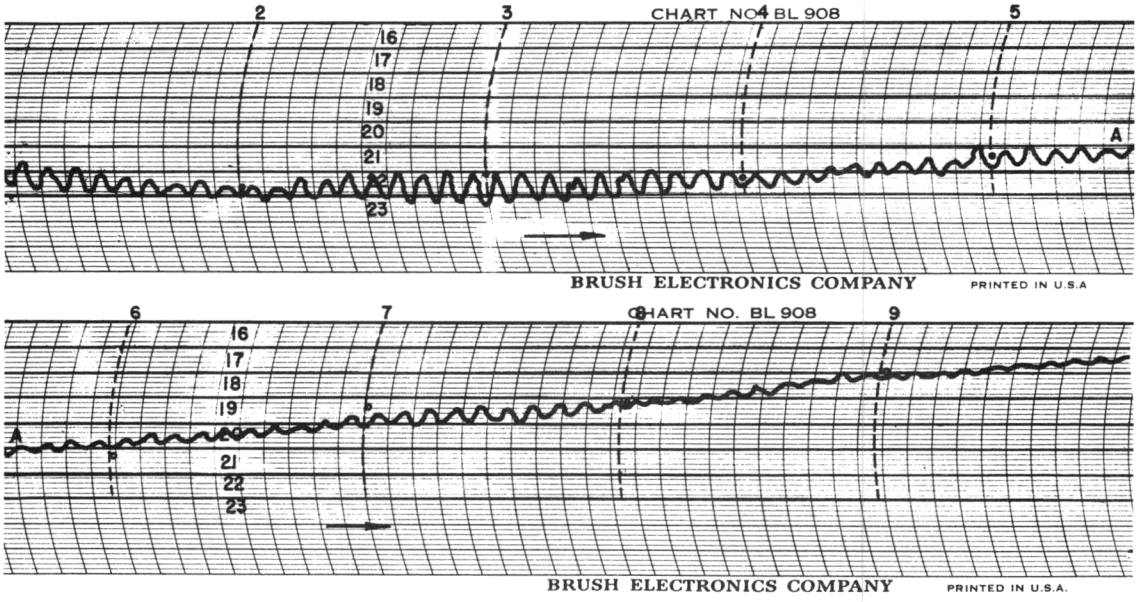

Figure 19

A Pen Recording of the Cladding Thickness of a Rod

B. An Eddy Current Testing Instrument for the Determination of Zirconium Wire Quality

1. Introduction

The design of the EBR-I Mark III reactor included zirconium wire spacers for the fuel elements. An eddy current technique was used to check the quality of the zirconium wire for cracks and voids. The instrument used was a modification of the instrument discussed in Chapter III of ANL-5861, except that only the amplitude variations of the bridge output were used. A block diagram of the eddy current instrument is shown in Figure 20.

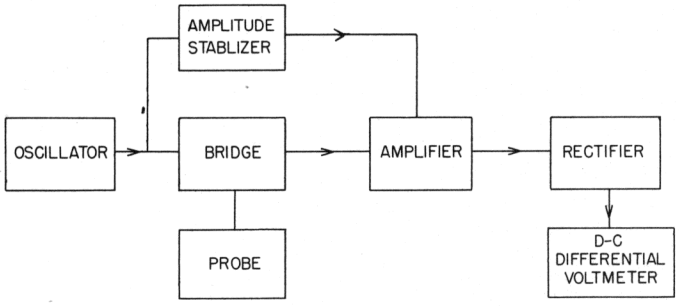

Figure 20

Block Diagram

There were several possible tests to determine the quality of the wire. First a visual examination was used to locate surface defects. This system was slow, and the nature of the external defect did not give a description of internal defects. Ultrasonics has been widely used for detecting internal defects, but in this particular application the small diameter (0.055 inch) of the wire prohibited the use of this test.

2. Theory

A small test coil establishes a magnetic field in the wire to be tested. This magnetic field induces eddy currents in the wire. The magnitude and direction of the eddy currents depends upon the test coil geometry, the coil excitation voltage amplitude and frequency, the distance from the coil to the wire, and the electrical properties and quality of the wire. The impedance of the coil changes with a variation of the magnitude and direction of the eddy currents.

Measurements of the change in impedance of the coil can provide information concerning any of the above parameters. In this application, the wire quality was the only variable. Determination of the other parameters will be discussed later in this paper. Test coil sensitivity is the magnitude of the impedance change for a standard defect. This can also be defined in terms of the bridge output voltage. Coil definition is inversely related to the volume covered by the eddy currents.

Maximum sensitivity and definition usually are desired in any test. Coil geometry largely determines the sensitivity and definition; however, the maximum for each variable does not occur for one particular coil geometry. A compromise must be made in accordance with testing problems. The optimum coil geometry is determined experimentally.

There are two types of test coils. The first type is called a point probe, because the axis of the coil is perpendicular to the surface of the conductor to be tested. In the ideal situation the source of the magnetic field would be a point, but in the actual situation a definite area is covered by the coil. This type of coil is used when the conductor to be tested has a flat surface or a diameter which is larger than coil diameter. The second type of test coil is called an encircling coil because the coil encircles the conductor to be tested. The eddy currents cover the volume of the conductor which is inside the coil. This type of coil is used when the conductor to be tested has a small diameter or a small cross-sectional area. Each of these two coil types have advantages over the other type in applications to particular problems. The proper type of coil is determined experimentally. An encircling coil was used for testing the zirconium wire.

3. Operation

The change in the impedance of the test coil was measured by the modified Owens bridge circuit shown diagrammatically in Figure 21. The circuit was composed of the test coil, two variable resistances, and two fixed capacitances. The two variable resistances were used for the final balancing of the bridge. Determination of the capacitance values will be discussed later.

The bridge was balanced with the coil in air. When a wire was brought near the coil, an unbalanced voltage appeared at the output terminals of the bridge. This voltage contained information about the defects in the wire. The crystal-controlled oscillator shown in Figure 21 supplied a 20-volt peak-to-peak sinusoidal voltage to the primary winding of the LS-30 transformer. The variation in this voltage was ± 15 millivolts. This drift could have led to a considerable error in the results, so the amplitude-stabilizing circuit shown in Figure 21 was used to eliminate practically all the error. In the stabilizing circuit, the voltage at the transformer input was rectified, and a portion of this rectified voltage was applied as a bias voltage on the grid of the first stage of the amplifier. When the correct amount of bias was added, the oscillator voltage could be varied over a considerable range without introducing a change in the amplifier output voltage.

The unbalanced voltage from the bridge circuit was amplified with the five-stage amplifier shown in Figure 21. A tuned circuit from the grid of the second stage to the ground was employed to eliminate the

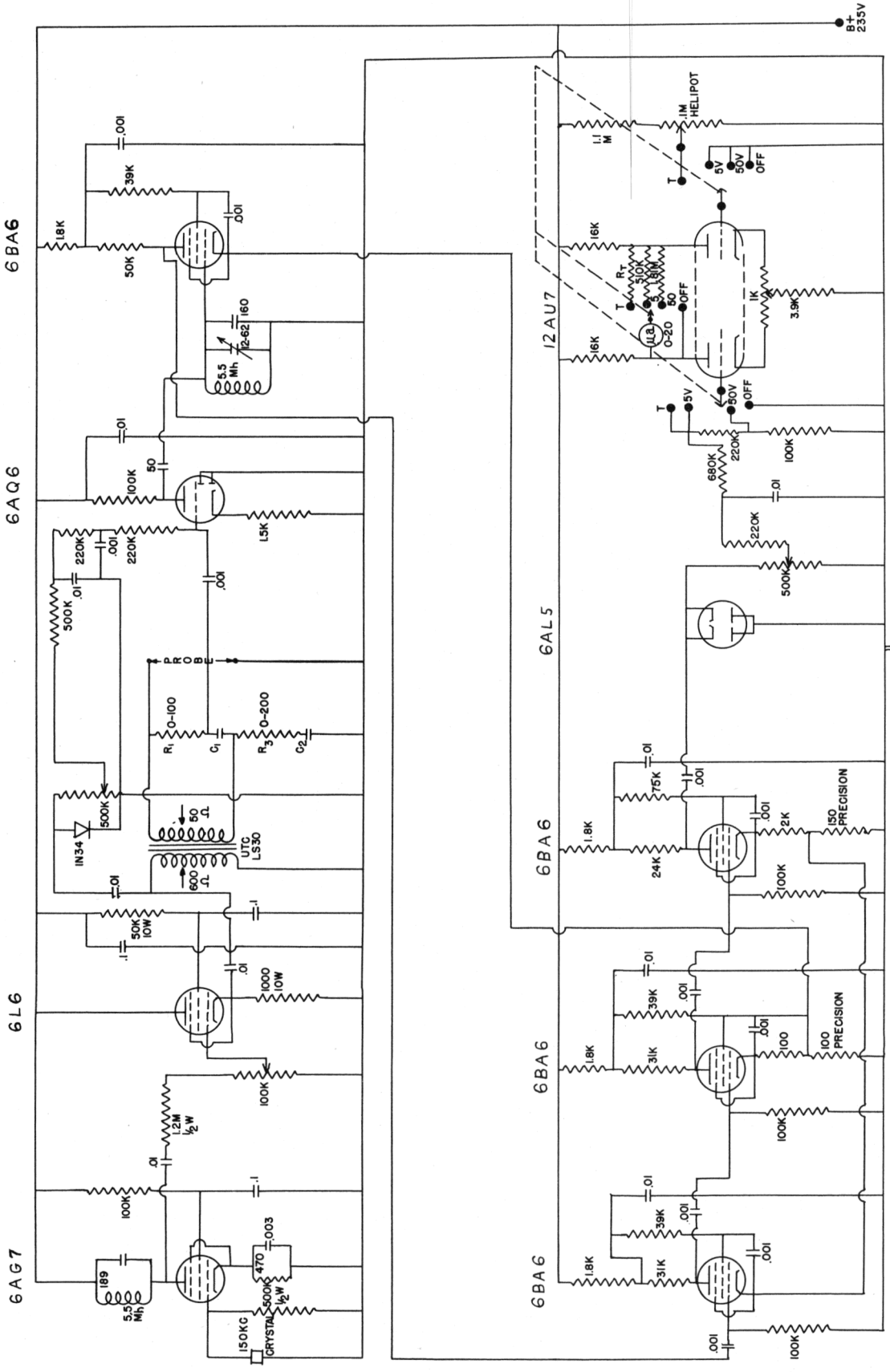

Figure 21

Circuit Diagram

undesirable harmonics. The last four stages were coupled, by several degenerative feedback loops, to improve the stability. The amplifier output voltage was rectified and the DC output voltage was adjustable with the 500-kilohm variable resistance. The differential DC voltmeter in Figure 21 indicated the output voltage. The 50 and 5-volt scales were used for balancing the bridge and adjusting the output voltage for a given condition of unbalance. The test (T) scale was used for indicating the wire quality. When the meter was on the test scale, the variable resistance in the grid circuit of the 12AU7 balanced out a portion of the DC voltage. This allowed the remaining DC voltage to cover the entire meter range; thus the meter deflection was greatly increased for a given defect in the wire. A photograph of the complete instrument is shown in Figure 22.

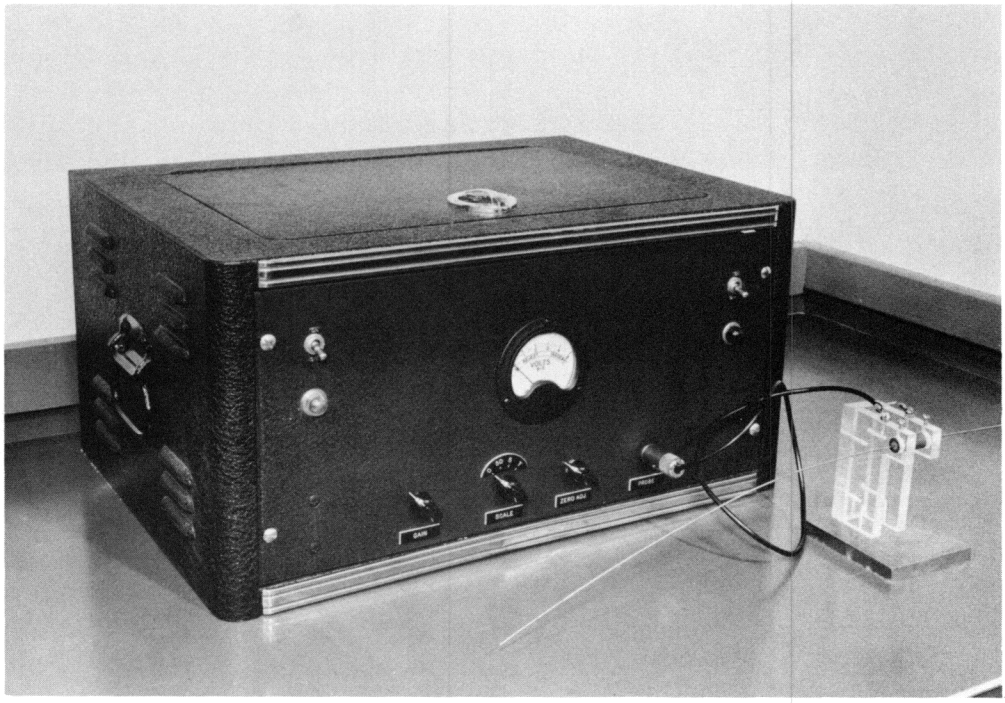

Figure 22

Photograph of the Completed Instrument

4. Application

The following procedure was used in testing the zirconium wire for cracks and voids. This is a typical application, and the procedure outlined here can be followed in other applications for which this instrument can be utilized. The most important factor in determining the coil type was the diameter (0.055 inch) of the zirconium wire. The point probe could not be made small enough for good sensitivity; however, the encircling coil proved to be very effective for detecting the cracks and voids. The cross section of this coil is shown in Figure 23 and a photograph of the coil is shown in Figure 22. Several different diameters, lengths, and number of turns were tried for the coil to obtain optimum sensitivity and definition.

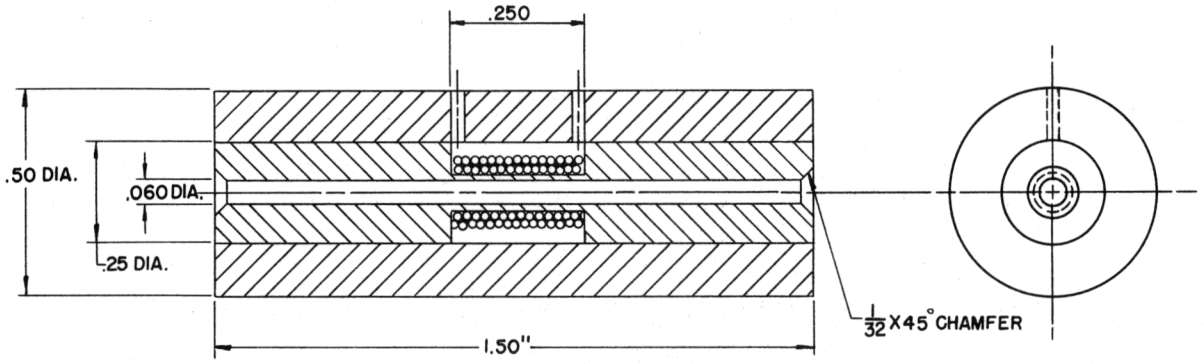

SCALE = 4-1

Figure 23

Test Coil Cross Section

The diameter of the coil that was used was about 0.015 inch greater than the wire diameter. The coil was close to the wire, and this greatly improved the sensitivity. The length of the coil was 0.188 inch. Since the length affected both the sensitivity and definition, this length was a good compromise for this application. The coil had two layers of number 40 wire wound on a nylon coil form.

Variations in probe coil-to-wire spacing changed the impedance of the coil, and an error was introduced. To minimize this error, the diameter of the center hole of the probe was made 0.005 inch greater than the nominal wire diameter. Essentially no error was introduced for a variation of this magnitude. A change in wire diameter had about the same effect as a change in spacing. The diameter of this wire varied $\pm$ 0.003 inch, and again no appreciable error was introduced. Changes in the operating temperature of the coil varied its impedance. If these changes were too drastic, the calibration of the instrument was affected. These changes in temperature came from changes in the ambient temperature or from excess coil current. Eddy currents of a considerable range of frequency were satisfactory for detecting flaws in the wire. This range can be determined theoretically or experimentally, and it varies with the permeability, conductivity and diameter of the wire to be tested.

The bridge output voltage amplitude for a wire without defects was largely determined by the bridge parameters. A maximum output voltage was desired. This maximum output voltage was attained by

varying the ratio of C_1 to C_2. The capacitances C_1 and C_2 were determined experimentally for each coil. The correct values for the coil in this application are shown in Figure 21. Since the magnitude of the impedance change of the coil depended upon the electrical properties of the wire, the output voltage of the instrument also depended upon these properties. The electrical properties of the zirconium were fairly constant and no complications were introduced.

The defects in the wire appeared as cracks or voids along the length of the wire. The size of the crack or void determined the magnitude of the unbalanced voltage at the bridge terminals. The magnitude decreased as the size of the defect increased. Several typical cross sections of wire and corresponding meter readings are shown in Figure 24. A cross section of the standard wire is shown in Figure 25. The first two cross sections in Figure 24 were not etched, and this accounts for the smooth appearance of their surfaces.

To calibrate the meter test (T) scale, several wires were checked, and a complete range of voltage readings was obtained from the rectifier output. The wires were then sectioned at the points where the readings were taken, and the wire quality was determined. This gave two ranges of output voltage; 0.0 to 4.25 volts for the unacceptable wire, and 4.25 to 5.0 volts for the acceptable wire. To expand the range of acceptable wire, the test scale was calibrated for a full range of 2.5 volts. The value of the resistance (R_T) for this calibration was 0.2 megohm. The balancing adjustment in the meter circuit balanced out the undesirable 2.5 volts.

The procedure used to set up the instrument for operation contained these steps: The bridge was balanced with no wire in the test coil. With the meter on the 5-volt scale, the standard wire which was without defects was placed in the coil. The gain was adjusted until the meter read 5 volts. The meter was switched to the test scale, and the balance was adjusted until a full-scale deflection of the meter was obtained. The instrument was then ready to check wire.

The velocity of the wire through the probe was limited by the inertia of the meter needle. When the velocity was too great, the needle would not follow the output voltage and error was introduced. The velocity was approximately 1.5 inches per second in this application. This velocity can be greatly improved if the meter is replaced by an electronic relay circuit.

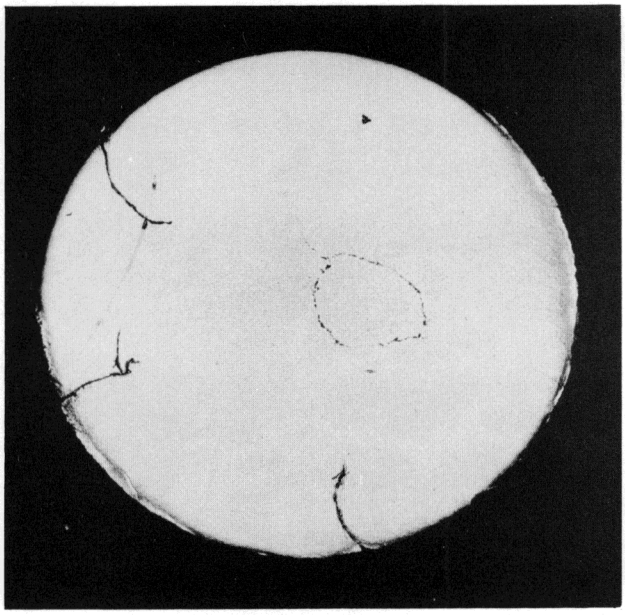

	METER READING
STANDARD WIRE	5.0
TEST WIRE	0.0

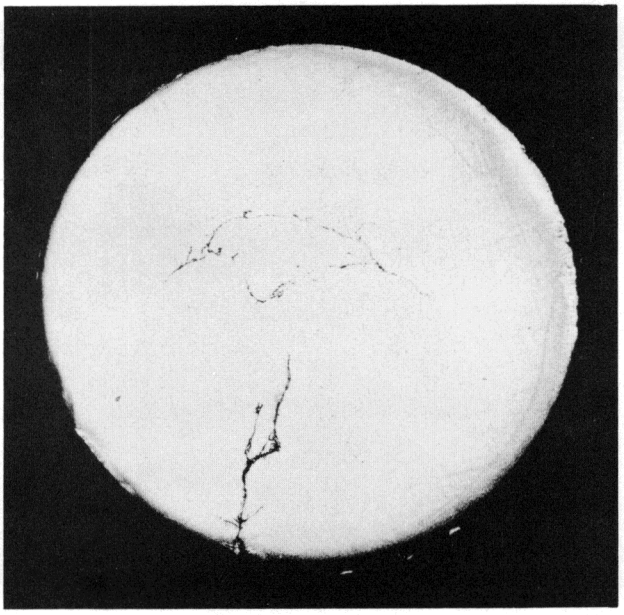

	METER READING
STANDARD WIRE	5.0
TEST WIRE	0.5

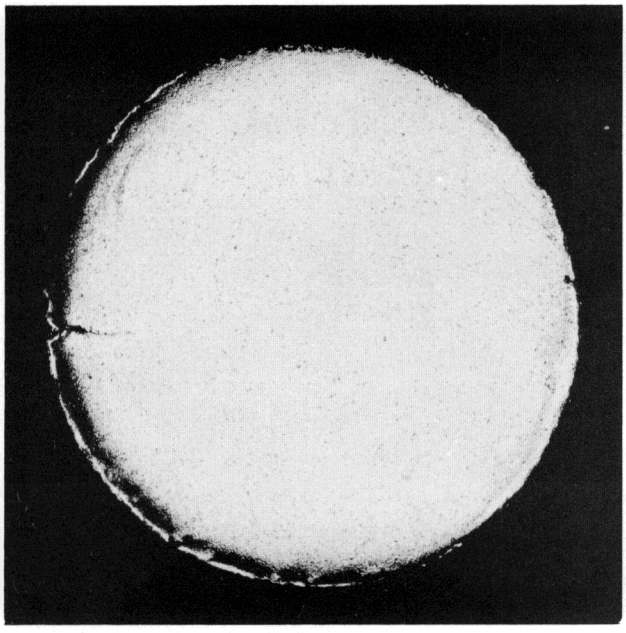

	METER READING
STANDARD WIRE	5.0
TEST WIRE	2.0

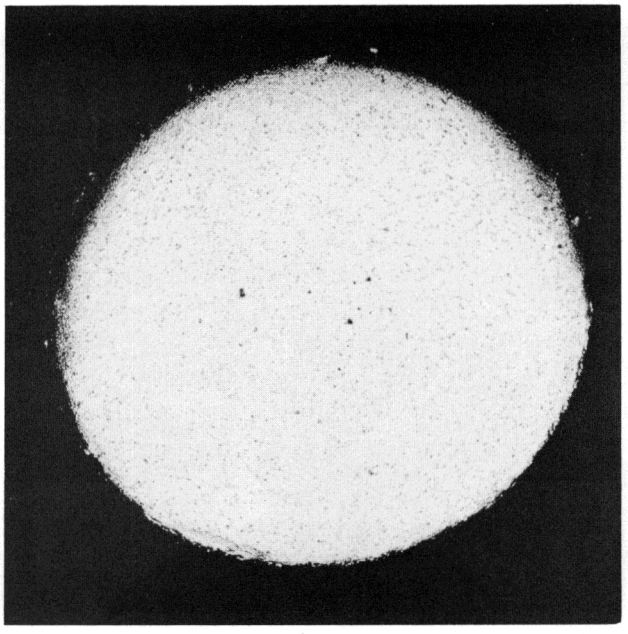

	METER READING
STANDARD WIRE	5.0
TEST WIRE	2.5

Figure 24

Wire Cross Sections and Corresponding Meter Readings

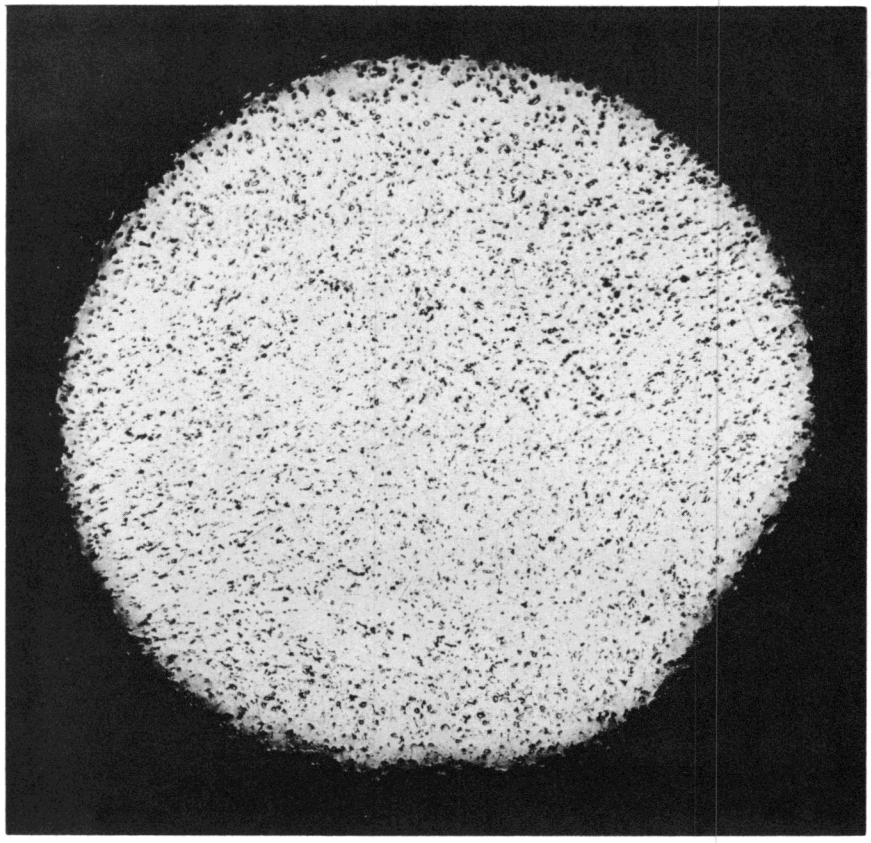

METER READING

STANDARD WIRE 5.0

Figure 25

Standard Wire Cross Section

5. Conclusion

Several hundred feet of wire were checked, and approximately 33 per cent was found to be acceptable. The final test of the wire was the spot welding and machining process. The accepted wire passed this test. This instrument can be depended upon to give a measure of the integrated wire quality; for example, several small cracks may give meter indication that is the same as one large crack. In the application described here, wire was rejected for small voids and porosity as well as for cracks. In production applications similar to the one described in this paper, the instrument can determine the quality of wire quickly and with good reliability.

REFERENCES

(1) J. H. Kittel, "Irradiation of Extrusion Clad Core Alloy for EBR-I Mark III," ANL-5918.

(2) H. F. Sawyer, "Coextrusion of Zircaloy-clad U-2 w/o Zr Rod for the EBR-I Mark III Core Loading," Nuclear Metals, Inc., NMI-4801.

(3) R. E. Macherey, N. J. Carson, Jr., R. L. Salley, and R. A. Beatty, "Fabrication of Fuel and Blanket Rod Stock for EBR-I Mark III," ANL-5895.

(4) R. A. Noland, C. C. Stone, F. D. McCuaig, and D. E. Walker, "The Manufacture of EBR-I Mark III Fuel and Blanket Rods," ANL-5917.

(5) W. N. Beck, and W. J. McGonnagle, "Development of Ultrasonic Techniques for Inspecting Experimental Boiling Water Reactor Cast Uranium Alloy Cores and Fuel Plates," ANL-5653 (December 1957).

(6) J. D. Ross, and R. W. Leep, "Ultrasonic Transmission Tester," The Journal of the Society for Nondestructive Testing, May-June, 1957.

(7) C. J. Renken, R. G. Myers, and W. J. McGonnagle, "Status Report in Eddy Current Theory and Application," ANL-5861, (April 1958).

APPENDIX A

INSPECTION STATISTICS ON EBR-I, MARK III FUEL ELEMENTS AND COMPONENTS

Number of castings tested - 109		
Number of fuel elements tested for nonbond - 832	3	defective
Number of section bonds inspected - 2,148	83	defective
Number of reprocessed and re-inspected defective section bonds - 83	2	defective
Enriched fuel rod tested for cladding thickness - 175 feet	4%	failed
Fuel blanket rod tested - 300 feet	5%	out of tolerance
Blanket rod tested - 1000 feet	3%	out of tolerance
Spacer wire checked - several hundred feet	67%	rejected